IOP Conf. Series: Materials Science and Engineering **655** (2019) 012004 doi:10.1088/1757-899X/655/1/012004

Effect of intercritical annealing of normalised Nb-Ti-V microalloyed plate steel on microstructural evolution

PI Kambilinya[1, a], CW Siyasiya[1, b], KM Banks[1, c], RJ Mostert[1, d]

[1] University of Pretoria, Department of Materials Science & Metallurgical Engineering, Pretoria, 0002, South Africa

E-mail: [a] pkambilinya2@gmail.com

Abstract. A homogeneous microstructure is required for consistent mechanical properties in normalised Nb-Ti-V microalloyed plate steels. Frequently, as-hot rolled microalloyed plate steels have a banded microstructure that is persistent even after normalising heat treatment (NHT), and this leads to inconsistencies and some scatter in mechanical properties. Therefore, this work focused on the influence of single-cycle normalising heat treatment (SNHT), double-cycle normalising heat treatment (DNHT) followed by intercritical annealing normalising heat treatment (INHT) on the homogenisation and mitigation of a banded microstructure. The study was conducted on a *0.13C-Nb-Ti-V* plate steel grade. The as-hot rolled microstructure was banded and had a 1.13 Anisotropy Index (AI) value. Results from the three thermal cycles revealed that the DNHT and INHT mitigated the pearlite microstructural banding and gave a more homogenized pearlite phase distribution throughout the microstructure, unlike the SNHT that retained the banding. The DNHT also exhibited the finest ferrite grain size, while the INHT exhibited the coarsest. From Vickers hardness measurements (153±5.8 HV, 157±3.6 HV and 166±4.5 HV), the UTS was approximately deduced as, 480, 490 and 530 MPa for the SNHT, DNHT and INHT respectively.

1. Introduction

A well-known phenomenon called microstructural banding usually occurs in hot-rolled microalloyed steels. This usually originates from the cast slab during dendritic solidification and/or solid-state phase transformations governed by microsegregation which then develops into a banded microstructure [1]–[3]. Microstructural banding has negative effects on the ductility and the impact toughness of microalloyed steels [4], [5]. It is reported that microstructural banding's severity and persistence due to prior microstructure memory is dependent on the rate of cooling, prior austenite grain size, and austenitising temperature [6], [7]. It was also reported that, even though high cooling rates (~ 60°C s^{-1}) during hot rolling eliminated banding, it reappeared after a separate post hot rolling intercritical treatment [3]. This behaviour of microstructure banding reversion (memory) was also investigated in a short time-high temperature normalising heat treatment (NHT), and it was reported that microsegregation was the root cause for the reappearance of the banding [5]. Therefore, this work focuses on studying the microstructural behaviour after NHT with the aim of mitigating microstructural banding and memory in a Nb-Ti-V microalloyed steel.

2. Experimental Procedure

The chemical composition for the 30 mm thick Nb-Ti-V microalloyed steel used in this study is given in Table 1**.** The plate was hot-rolled from 240 mm thick slabs, and the finishing rolling temperature was 860 °C followed by cooling in air.

Table 1. Chemical composition of the experimental steel, mass-%.

	Chemical element											
Steel	**C**	**Mn**	**P**	**Si**	**Ni**	**Cr**	**V**	**Nb**	**Al**	**Ti**	**N**	**Fe**
Nb-Ti-V	0.13	1.5	0.014	0.4	0.03	0.03	0.03	0.043	0.04	0.025	0.0053	Bal.

Thermo-Calc® 6.0 software, Steel and Iron Alloys Database TCFE7, was used to predict the equilibrium ferrite to austenite phase transformation temperature, Ac_e. The dilatometer specimens were wire cut from the centre of the as-hot rolled steel to a height of 10 mm and a diameter of 5 mm. An inductive Bähr dilatometer (DIL 805A/D) was used to experimentally determine the Ac_3 temperature in accordance with ASTM A1033-18. The normalising schedules in Figure 1, were also performed on the Bähr dilatometer. Macro and micro Vickers hardness tests were then conducted on the heat treated samples.

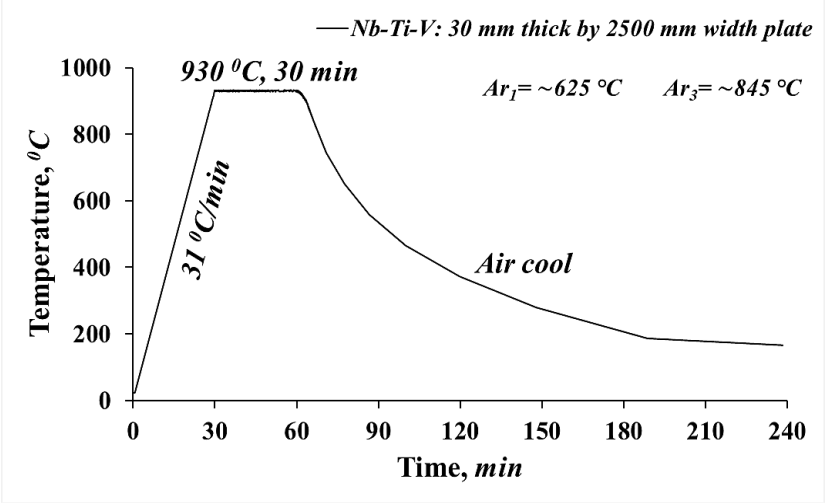

(a)

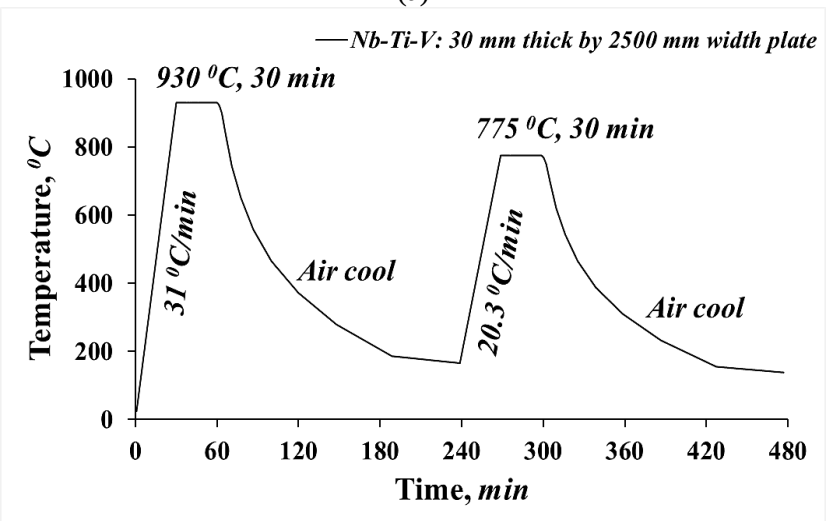

(b)

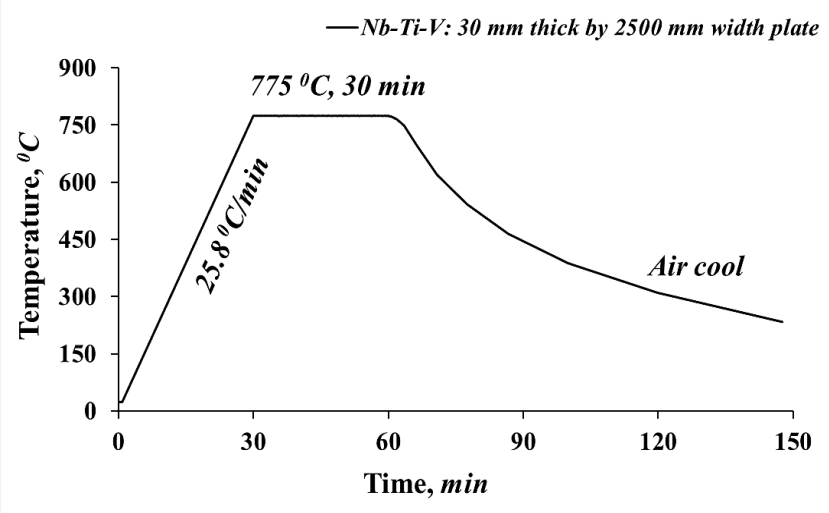

(c)

Figure 1: Applied heat treatment cycles: **(a)** single-cycle solution treatment (SNHT) in the austenite phase region at 930°C for 30 min then cooling in air; **(b)** double-cycle solution treatment in the austenite phase region at 930°C for 30 min and air cooling followed by an intercritical treatment at 775°C for 30 min and air cooled (DNHT); **(c)** intercritical treatment 775°C for 30 min and cooling in air (INHT).

Metallography was performed on both the as-hot rolled and the heat-treated samples using an *Olympus BX51M* optical microscope. With the aid of *Image J*® software, ferrite and prior austenite grain sizes (PAGS) were determined. The ferrite grain size distribution and the extent of banding were measured and quantified in accordance with respective ASTM standards: ASTM E112-13, ASTM E 1268-01, and ASTM E 562-11. The ferrite grain size distribution from the surface to the centre of the steel plate was calculated by means of the *Heyn's Lineal Intercept Procedure* [8], with test lines yielding at least 50 intercepts. The main parameters used to quantify and characterize the extent of banding in the steel's microstructure are: anisotropy index (AI); centre-to-centre mean spacing of the banded phase ($SB_{\perp}$); edge-to-edge mean free path spacing of the banded phase ($\lambda_{\perp}$); and the mean width of the banded phase given by calculating the difference between the mean spacing and the mean free spacing, Table 2. The two mean quantities give a measure of the number of bands per mm. The AI indicates how banded a matrix is, i.e., a non-banded matrix will have an AI of 1; as the degree of banding increases, so does the AI value above 1.

Through-thickness, as-rolled samples were austenitised at temperatures between 965 and 1050°C for 2 hours followed by quenching in water (at room temperature). The PAGS were determined using the lineal intercept procedure as described in ASTM E112-13.

3. Results and Discussion

3.1. As-hot rolled and PAGS microstructure analysis

Microstructural banding

According to ASTM E1268-01, Standard Practice for Assessing the Degree of Banding or Orientation of Microstructures, by observation of the optical morphology, a banded microstructure can be defined as: "the separation, of one or more phases or constituents in a two-phase or multiphase microstructure or constituent microstructure, into distinct layers parallel to the deformation axis due to elongation of microsegregation" [2]. The extent to which the as hot-rolled microstructures were banded is summarised in Table 2.

Table 2. The extent of microstructural banding in as-hot rolled 30 mm thick plate

	Nb-Ti-V Steel			
	NS[a]	**QT[b]**	**MT[c]**	**AVERAGE**
Mean, $\bar{X}$	17.1	15.6	15.2	**16**
SD	2.57	2.92	1.71	**2.4**
%RA	11	14	9	**11.3**
95% CI, ±	1.94	2.2	1.29	**1.81**
AI	1.07	1.21	1.1	**1.13**
$SB_{\perp}$, μm	69.3	71.5	77	**72.6**
$\lambda_{\perp}$, μm	46.4	47.2	53.9	**49.2**
($SB_{\perp}$ - $\lambda_{\perp}$), μm	22.9	24.3	23.1	**23.4**

[a] *Near-surface*
[b] *Quarter-thickness*
[c] *Mid-thickness*

From the quantitative analysis results in Table ***2***, the ferrite AI value (greater than 1), confirmed that the ferrite grains and the pearlite colonies were oriented in the direction of rolling. Hence, the presence of the parallel and layered ferrite-pearlite microstructure. The other banding spacing parameters ($SB_{\perp}$ and $\lambda_{\perp}$) give an insight of the distances between the bands.

Ferrite grain size distribution.

The ferrite grain size was unevenly distributed; increasing from the surface to the centre, Figures 2a-c show micrographs of ferrite (light phase) and pearlite (dark phase) at the surface and the centre respectively, together with the respective mean and standard deviations of ferrite intercept length, $\bar{l}_{\alpha}$.

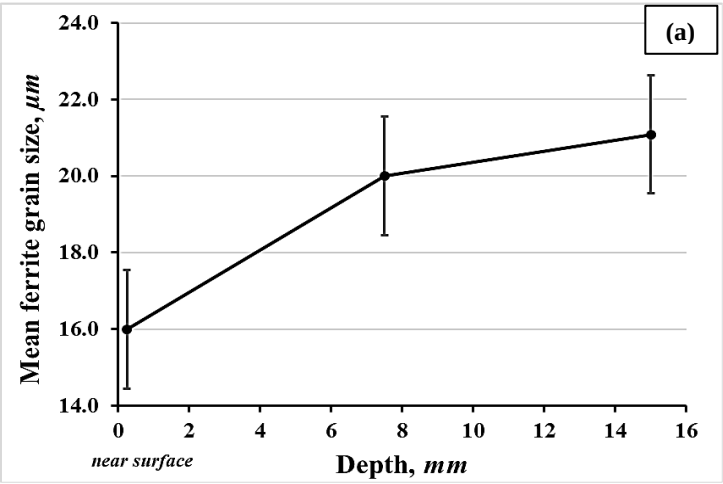

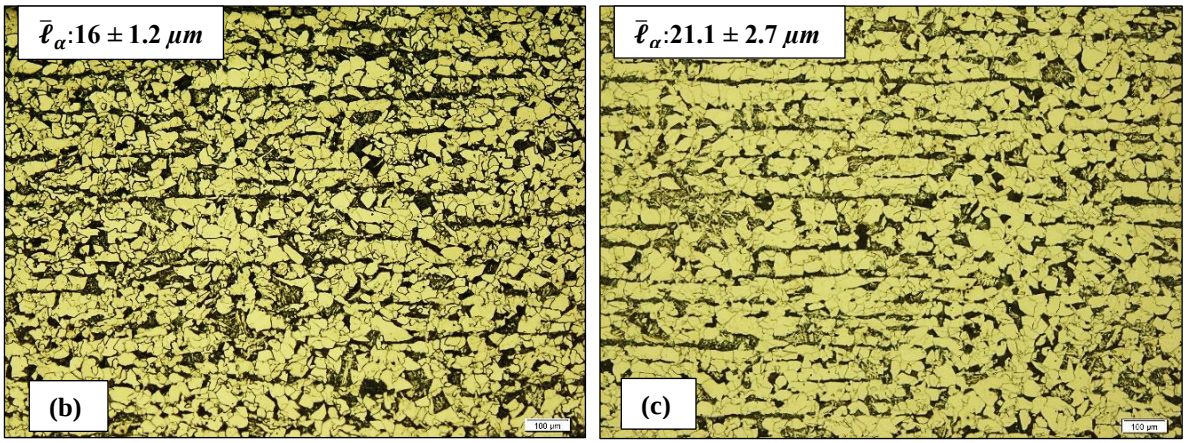

Figure 2. (a) Ferrite grain size distribution in as-hot rolled condition measured across the plate cross-section; (b) near to the surface; (c) at mid-thickness. Scale bar 100 μm, images taken in the rolling direction.

Characterisation of the prior austenite grain size (PAGS)

Figure 3 shows that the PAGS increased from the surface to the centre. Also, the PAGS difference between surface and centre becomes more pronounced at higher austenitising temperatures. Evidently, this shows some memory retention by the microstructure even after austenitisation.

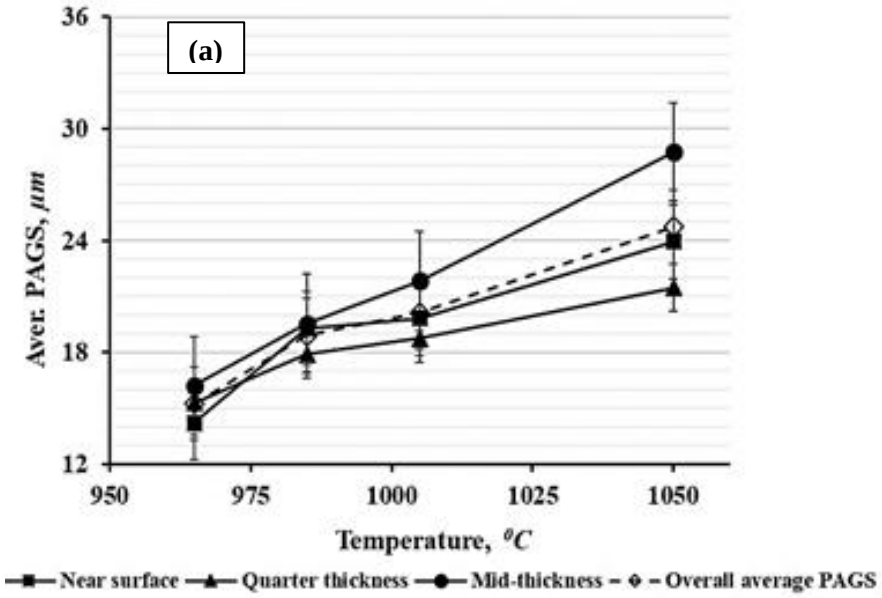

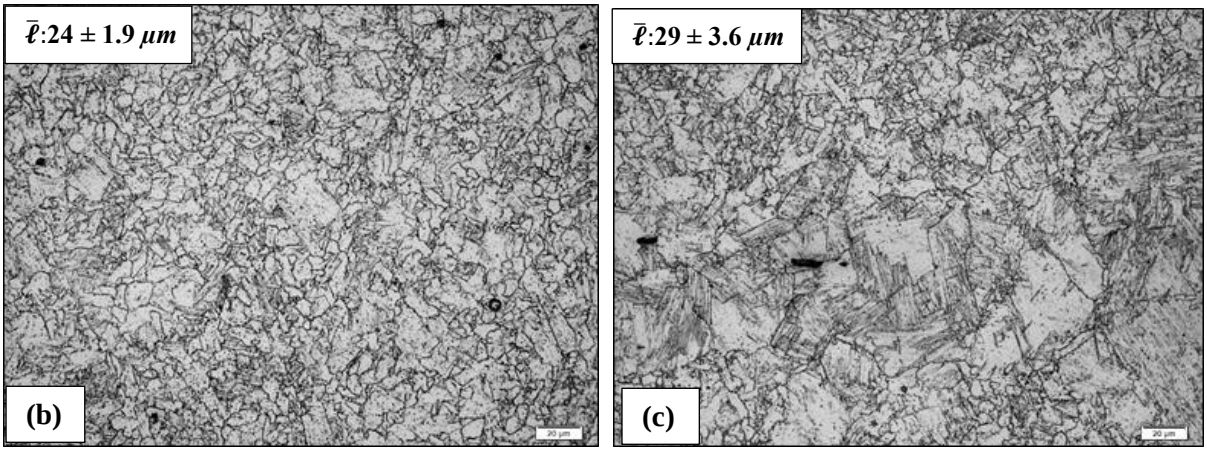

Figure 3. Micrographs of PAGS showing grain size distributions: (a) Average PAGS vs austenitising temperature. Soaked for 2hrs followed by water quenching to room temperature; (b) taken near to the surface; (c) at mid-thickness. Austenitised at 1050 °C for 2hrs followed by water-quench, then tempered at 496 °C for 26 hrs. Scale bar 20 μm.

3.2. Normalising heat treatment simulations and microstructure analysis

The hot-rolled banded structure was still present even after the 930°C for 30 min single-cycle normalising heat treatment (SNHT) simulation, Figure 4a. The microstructures after the double-cycle normalising heat treatment (DNHT), Figure 4b, and to some extent the intercritical-anneal normalising heat treatment (INHT) in Figure 4d appears to mitigate the ferrite-pearlite banded structure. Nonetheless, the INHT resulted in a coarser microstructure (ferrite) than the DNHT. The DNHT has, however, been reported to produce similar YS and UTS values compared to the SNHT [9]. During heating and austenitising in SNHT diffusion-controlled nucleation of austenite occurs predominantly at ferrite-pearlite colony interphases (i.e. sites of higher carbon concentrations). As the cementite lamellae in the pearlite dissolve, carbon and other alloying elements such as manganese [10]–[12], redistribute and attempt to homogenise in the austenite matrix. Upon air cooling from the austenite single phase region, pearlite transformation starts at the boundaries of ferrite and austenite and spreads into the austenite grains. The retention of the austenite morphological structure therefore, results in a banded pearlitic structure upon air cooling as evidenced in Figure 4a.

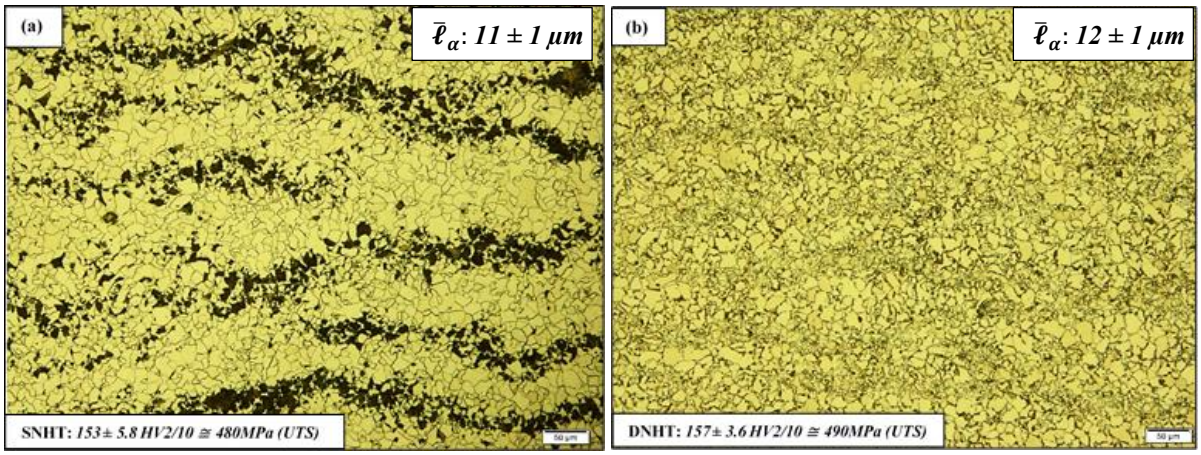

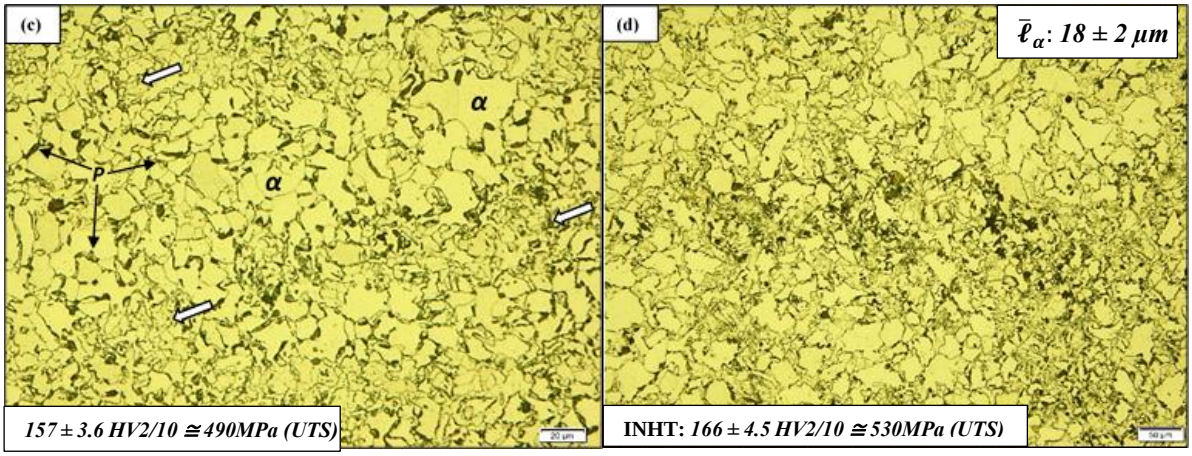

Figure 4: (a) SNHT, scale bar 50 μm; (b) DNHT, scale bar 50 μm; (c) same as in (b), taken at higher mag. (scale bar 20 μm) to show fine pearlite nodules nucleating at ferrite grain boundaries and corners. Also note, fine pearlite nucleating in the carbon-rich regions (large arrows); (d) INHT, scale bar 50 μm.

Table 3: Ferrite, pearlite micro Vickers hardness, and pearlite vol. fraction with respective HT.

	Heat Treatment Type		
	SNHT	**DNHT**	**INHT**
Average (ferrite), *HV*	176.1 ± 13.8	181.1 ± 5.1	189.6 ± 12.3
Average (pearlite), *HV*	229 ± 10.8	260 ± 23.1	272 ± 12.4
Vol. fraction (pearlite), %	39	30	32

During intercritical annealing upon heating and soaking, austenite formation takes place only in the carbon-rich regions that featured pearlite [13], thereby only dissolving the banded pearlite regions, this can be noted in the post intercritical annealing of the DNHT, Figure 4c pointed with large ***arrows***. Upon air cooling the carbon enriched austenite is significantly stabilised and subsequently delays the pearlite transformation and is extremely important for intercritical heat treatments [11]. Furthermore, cooling from the intercritical (α+γ) region fosters the epitaxial growth of new and fine ferrite grains at already existing ferrite interfaces [14], Figure 4c. Epitaxial ferrite, as defined by Sarwar et al. [15], is "ferrite formed by the transformation of austenite by epitaxial growth on retained ferrite (ferrite present at intercritical annealing temperature) during cooling from intercritical annealing temperature". This mechanism further enriches the surrounding austenite with carbon. Thus, cooling of austenite from the intercritical region delays the pearlite transformation compared to cooling from the single γ-phase region. Evidently, in Figure 4c the large arrows show the carbon-rich regions that had stabilised the austenite and resulted in the delayed pearlite transformation, thereby mitigating the pearlite bands after air cooling.

It was also observed in another study that while austenite enrichment with carbon delayed the austenite to pearlite transformation, it, however, increased the starting temperature of ferrite formation [16]. This explains why there is an increase in the volume fraction of ferrite, and finer pearlite as depicted in Figure 4b. Moreover, a progressive ferrite grain refinement and homogeneity in terms of pearlite distribution was observed with an increase in the number of NHT cycles.

In comparison to the SNHT and DNHT, despite being conducted at a lower temperature the INHT produced larger ferrite grains, Figure 4d. This could also have been attributed to the growth of the retained ferrite during the intercritical annealing. This is not the case with the SNHT and DNHT, where there was complete transformation to austenite during austenitisation; the ferrite grains had been refined upon air-cooling. This has also been reported by Chatterjee et al., [17]. Although the DNHT also

involved intercritical annealing, the growth of retained ferrite was not as pronounced as in the INHT due to the initial cycle.

The INHT, however, produced microstructure with slightly the highest HV values despite having larger ferrite grains. This could have resulted from the refined pearlite which is slightly in higher volume fraction in the INHT than the other two heat treatments, Table 3. This can be supported by another similar study [18]. In addition, the austenite that is formed during intercritical annealing in the INHT relatively contains a higher carbon content due to the pearlite-austenite transformation as opposed to that in the DNHT. Upon transformation after air-cooling, it appears as though the INHT produced regions of ferrite with higher carbon content which contributed to the strengthening. The high austenitisation temperature in the initial cycle of the DNHT resulted in a higher carbon content partitioned to the austenite phase [11], [19]. This factor, though, is subject to further investigation.

4. Further work

This work addresses the mitigation of microstructural banding and its memory retention by investigating the effect of the DNHT and INHT on the as-hot rolled microstructure. However, more experimental work that investigates the effect of austenitisation temperature on the microstructure banding (memory retention) in the SNHT needs to be conducted. In addition, further investigation on the effect of the applied heat treatments on the mechanical properties such as; yield strength, CVN impact energy absorption and the ductile-to-brittle transition temperature (DBTT) also needs to be done.

5. Conclusions

- The double normalising heat treatment involving an intercritical austenitisation after normalising followed by air cooling mitigates the pearlite microstructural banding and homogenizes the pearlite phase distribution throughout the microstructure.
- The double normalising heat treatment further refined the ferrite grain size upon γ-decomposition during air cooling from the intercritical region. This heat treatment possibly had no impact on tensile strength as confirmed by Vickers hardness measurements.

6. References

[1] S. Cai and J. D. Boyd, “Mechanism of Microstructural Banding in Hot Rolled Microalloyed Steels,” *Mater. Sci. Forum*, vol. 500–501, no. August, pp. 171–178, 2005.

[2] ASTM E 1268-01, “Standard Practice for Assessing the Degree of Banding or Orientation of Microstructures,” *Am. Soc. Test. Mater. Int.*, no. Reapproved 2016, pp. 1–29, 2016.

[3] F. G. Caballero, A. Garcia-Junceda, C. Capdevila, and C. G. de Andres, “Evolution of Microstructural Banding during the Manufacturing Process of Dual Phase Steels,” *Mater. Trans.*, vol. 47, no. 9, pp. 2269–2276, 2006.

[4] A. S. Bor, “Effect of Pearlite Banding on Mechanical Properties of Hot-rolled Steel Plates,” *ISIJ Int.*, 2008.

[5] R. A. Grange, “Effect of microstructural banding in steel,” *Metall. Trans.*, 1971.

[6] L. E. Samuels, *Light Microscopy of Carbon Steels*. 1999.

[7] T. F. Majka, D. K. Matlock, and G. Krauss, “Development of microstructural banding in low-alloy steel with simulated Mn segregation,” *Metall. Mater. Trans. A Phys. Metall. Mater. Sci.*, 2002.

[8] ASTM E112 − 13, "Standard Test Methods for Determining Average Grain Size," *Am. Soc. Test. Mater. Int.*, no. Reapproved 2014, pp. 1–28, 2014.

[9] T. F. Muniz, V. B. Trindade, and G. L. Farai, "Effect of Some Heat Treatments on Microstructure and Mechanical Properties of a Microalloyed Low Carbon Steel Aiming to Attend the Oil and Gas Industry," *Proc. 23rd ABCM Int. Congr. Mech. Eng.*, no. December, pp. 6–11, 2015.

[10] G. R. Speich, V. A. Demarest, and R. L. Miller, "Formation of Austenite During Intercritical Annealing of Dual-Phase Steels," *Metall. Mater. Trans. A*, 1981.

[11] N. Fonstein, *Advanced High Strength Sheet Steels*. 2015.

[12] S. ci Li, Y. lin Kang, G. ming Zhu, and S. Kuang, "Austenite formation during intercritical annealing in C-Mn cold-rolled dual phase steel," *J. Cent. South Univ.*, 2015.

[13] R. Großterlinden, R. Kawalla, U. Lotter, and H. Pircher, "Formation of pearlitic banded structures in ferritic-pearlitic steels," *Steel Res.*, 1992.

[14] M. D. Geib, D. K. Matlock, and G. Krauss, "The effect of intercritical annealing temperature on the structure of niobium microalloyed dualphase steel," *Metall. Trans. A*, 1980.

[15] M. Sarwar, E. Ahmad, K. A. Qureshi, and T. Manzoor, "Influence of epitaxial ferrite on tensile properties of dual phase steel," *Mater. Des.*, p. 335, 2007.

[16] O. A. Girina, D. B. Bhattacharya, N. M. Fonstein, "Effect of Annealing Parameters on Austenite Decomposition in a continuously Annealed {Dual-Phase} Steel," *41st {MWSP}*, no. January 2003, pp. 403–414, 2003.

[17] A. Chatterjee, D. Chakrabarti, A. Moitra, R. Mitra, and A. K. Bhaduri, "Materials Science & Engineering A Effect of normalization temperatures on ductile – brittle transition temperature of a modi fied 9Cr – 1Mo steel," *Mater. Sci. Eng. A*, vol. 618, pp. 219–231, 2014.

[18] M. P. Engineering and N. Unive, "Inter-critical heat treatment of a low-alloy steel," vol. 40, pp. 395–405, 1994.

[19] R. G. Davies and C. L. Magee, "Physical Metallurgy of Automotive High-Strength Steels.," *Journal of Metals*. 1979.